TRANSVERSE BEAM SPLITTING MADE OPERATIONAL: RECENT PROGRESS OF THE MULTI-TURN EXTRACTION AT THE CERN PROTON SYNCHROTRON

A. Huschauer*, J. Borburgh, S. Damjanovic, S. S. Gilardoni, M. Giovannozzi, M. Hourican, K. Kahle, G. Le Godec, O. Michels, G. Sterbini, CERN, Geneva, Switzerland
C. Hernalsteens, Ion Beam Applications, Louvain-la-Neuve, Belgium

Abstract

Following a successful commissioning period, the Multi-Turn Extraction (MTE) at the CERN Proton Synchrotron (PS) has been applied for the fixed-target physics programme at the Super Proton Synchrotron (SPS) since September 2015. This exceptional extraction technique was proposed to replace the long-serving Continuous Transfer (CT) extraction, which has the drawback of inducing high activation in the ring. MTE exploits the principles of non-linear beam dynamics to perform loss-free beam splitting in the horizontal phase space. Over multiple turns, the resulting beamlets are then transferred to the downstream accelerator. The operational deployment of MTE was rendered possible by the full understanding and mitigation of different hardware limitations and by redesigning the extraction trajectories and non-linear optics, which was required due to the installation of a dummy septum to reduce the activation of the magnetic extraction septum. The results of the related experimental and simulation studies, a summary of the 2015 performance analysis, as well as more recent performance improvements are presented in this paper.

INTRODUCTION

To provide high-intensity beams for fixed target physics at the SPS, the longitudinal structure delivered by the PS has to comply with certain requirements. In order to reduce beam loading and to provide an almost continuous spill towards the experimental facilities, uniform filling of the SPS is desired. Considering that the length of the SPS is about eleven times the circumference of the PS, and that a gap for the rise time of the SPS kickers is needed, the non-resonant CT process was proposed in 1973 [1]. This extraction technique, which occurs over five turns at 14 GeV/c, allows to optimize the duty cycle as only two subsequent extractions from the PS are necessary. On the downside, the CT extraction comes with the major drawback of significant beam loss occurring at multiple locations around the ring [2], leading to high dose to personnel during accelerator repair and maintenance as well as to long cool down times.

Therefore, the MTE technique was proposed to replace the CT process in 2001 [3]. MTE is a resonant extraction mechanism, which exploits advanced concepts of non-linear beam dynamics and applies a fourth order stable resonance to perform beam splitting in the horizontal phase space. The resulting beamlets - one core and four islands - are then extracted over five turns.

Due to the complexity of the MTE scheme, its operational implementation has had to overcome many challenges. In 2010, about one month of operational experience could be gathered with this novel technique, and two major issues were identified [4]:

(1) significant fluctuations in the efficiency of the transverse splitting, the losses at extraction and the trajectories in the transfer lines, and
(2) unacceptably high radioactive activation of the magnetic extraction septum (SMH16).

In order to overcome the second problem, a so-called dummy septum (TPS15), i.e. a passive absorber to shield SMH16, was developed and installed in straight section (SS) 15 of the PS during the Long Shutdown 1 (LS1) between 2013 and 2014 [5]. A certain fraction of the losses during the extraction is intrinsic to the process itself and the debunched longitudinal structure of the beam: during the rise time of the fast kickers, the continuous beam is swept from the internal to the external side of SMH16, causing unavoidable beam loss. Using TPS15, the activation of SMH16 can be reduced by relocating these losses from SS16 to the well-shielded SS15. It was only after the installation of this device that the MTE commissioning could be resumed.

In this paper, several experimental and simulation studies are presented, which allowed to increase the understanding of the MTE process and eventually led to the implementation of appropriate measures to overcome the two aforementioned problems. As a result of these studies, the MTE process was operationally deployed and has been used to deliver high-intensity beams to the SPS as of September 2015. Since then, it has successfully replaced the CT extraction [6].

Furthermore, an analysis of the MTE performance in 2015 and recent operational improvements, which aim at increasing the robustness of this extraction technique, are discussed.

PERIODIC OSCILLATIONS OF THE SPLITTING EFFICIENCY

The efficiency of the transverse splitting is the natural figure-of-merit of the MTE performance and is defined as

$$\eta_{\mathrm{MTE}} = \frac{\langle I_{\mathrm{Island}} \rangle}{I_{\mathrm{Total}}}, \qquad (1)$$

where $\langle I_{\mathrm{Island}} \rangle$ and I_{Total} stand for the average intensity in each island and the total beam intensity, respectively. The

* alexander.huschauer@cern.ch

ISBN 978-3-95450-178-6

nominal efficiency is 20%, corresponding to an equal beam sharing between islands and core. One of the challenges of working with transversely split beams is the fact that it is difficult to directly measure the locations of the various beamlets in the phase space. Therefore, η_{MTE} is inferred from phase space projections, which are obtained by using horizontal wire scanners (WSs).

Figure 1 shows the time evolution of several measured horizontal profiles. Clear oscillations of the intensities captured in the various beamlets are observed, with oscillation periods in the order of tens of minutes. This phenomenon caused cycle-by-cycle variations of η_{MTE} and, therefore, significant deviations from the minimum acceptable value of 19% set by the SPS.

Based on an extensive measurement campaign and subsequent simulation studies, the splitting process was understood to be significantly perturbed by a low-frequency modulation of the tune. The observed oscillations were actually caused by a current ripple introduced by the switch-mode power converters used to power the different circuits of the Pole-Face Windings (PFW), which are special auxiliary windings used to control transverse tunes and linear chromaticities [7]. The current ripple at the intrinsic frequency of these power converters of 5 kHz was found to be larger than expected and, more importantly, the lack of synchronization of the clocks of the different power converters resulted in a modulation of the tune at 5 kHz with varying amplitude in time. Figure 2 shows the excellent agreement between the time evolution of the measured profile amplitude of the outermost island (see Fig. 1) and the amplitude of the 5 kHz component of the PFW current.

Following a hardware intervention to reduce the current ripple at 5 kHz, the fluctuation of η_{MTE} was significantly improved. This achievement, which was the prerequisite to again transfer MTE beams to the SPS, is also visualized in Fig. 2, where the intensity of the different beamlets measured with a WS is shown to be constant in time.

By means of time-dependent 6D simulations with the PyORBIT code [8] - using PTC [9] as underlying tracking code - the effect of a tune modulation at 5 kHz on the efficiency of the transverse splitting was investigated. Therefore, the multipole elements required to perform the horizontal splitting, i.e. dedicated sextupole and octupole magnets, were programmed according to the operationally used values and the horizontal tune was constantly increased over 50×10^3 turns to cross the resonance and perform the transverse splitting. In addition, a 5 kHz tune modulation corresponding to the maximum measured ripple amplitude of the PFW circuits was included in the simulations. In Fig. 3, the resulting topology of the horizontal phase space is compared to the case

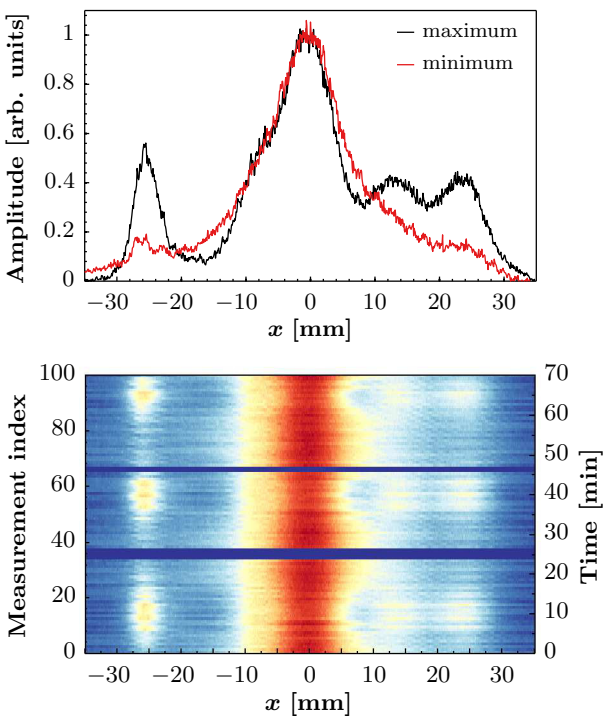

Figure 1: Top: Comparison between good and bad splitting efficiency based on measured horizontal profiles. Bottom: Waterfall representation of multiple measured horizontal profiles, with the colour scale corresponding to the amplitude of the data shown in the image at the top. Each measurement was recorded on a different cycle and clear oscillations of the beamlets' intensities are visible.

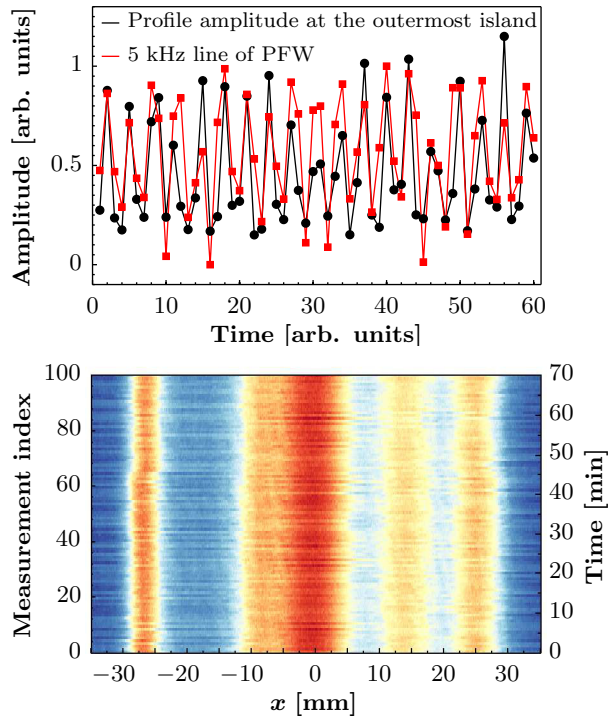

Figure 2: Top: Comparison between the time evolutions of the measured profile amplitude of the outermost island and the amplitude of the 5 kHz current ripple of the PFW. Bottom: Waterfall representation of multiple measured horizontal profiles after an intervention aimed at damping the PFW current ripple at 5 kHz. A significant improvement with respect to the measurements shown in Fig. 1 is clearly visible.

ISBN 978-3-95450-178-6

without any tune ripple. Due to the absence of the transverse damper, which is used to horizontally excite the beam for about 14×10^3 turns (the PS revolution period corresponds to 2.1 µs) after the crossing of the fourth order resonance at a frequency close to the resonant tune frequency to improve the trapping probability into the stable islands, simulations without any ripple show an efficiency of only 14%. However, similar experimental results of η_{MTE} were achieved without using the transverse damper, which highlights the very good capabilities of the non-linear model of the PS. Furthermore, a tune ripple was found to severely affect the splitting process, leading to a reduction of η_{MTE} by more than 1% for the chosen parameters.

Additional simulations, whose results are summarized in Fig. 4, revealed that the splitting efficiency is even more severely affected by frequencies lower than 5 kHz. For higher frequencies, however, the impact on the splitting was found to be less important. Furthermore, the secondary oscillation frequencies of the particles close to the stable fixed points (SFPs) inside the islands were understood to be in the low-kHz regime. Therefore, it was concluded that the depopulation of the islands in the presence of a low-frequency tune ripple occurs due to an overlap of the external excitation frequency with the particles' natural frequency of motion during the splitting process.

Based on the results of the presented studies, the feasibility of synchronizing the different power converters and of moving their switching frequencies to higher values are currently being investigated.

IMPROVED NON-LINEAR EXTRACTION OPTICS

Subsequent to the successful splitting in the horizontal phase space, the beamlets have to be rotated in order to correctly position them at SMH16. The results of the previously discussed time-dependent simulations revealed that the operationally used rotation process occurred very quickly and, therefore, non-adiabatically. Eventually, this results in filamentation and emittance blow-up, as the particles captured inside the islands are not able to follow the rapid motion of the SFPs (see Fig. 5).

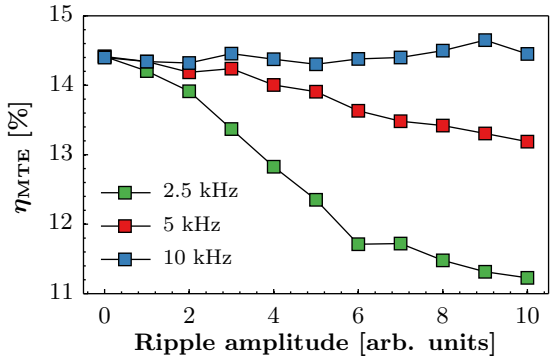

Figure 4: Dependency of the splitting efficiency on the frequency and amplitude of the external perturbation.

Further simulation studies with PTC led to the understanding that the surface of the islands can be reduced by properly choosing the multipolar configuration. Nevertheless, it has to be considered that any reduction of the surface is always accompanied by a certain probability of de-trapping [10]. This surface reduction in combination with the intended adiabatic rotation can eventually be achieved by acting either on the sextupolar or the octupolar component of the magnetic field. As acting on the octupolar component is accompanied by a significant change of the amplitude of the SFPs in the islands, it was decided to slowly adapt the sextupolar component to perform an appropriate rotation.

The results of simulations with an improved multipolar configuration are shown in Fig. 6. During the rotation, the islands follow the movement of the SFPs and slowly adapt to the new configuration. Thereby, they are elongated and the external one is reduced in horizontal size, which provides additional margin for the proper extraction process, as the clearance between the beam and the blade of the extraction

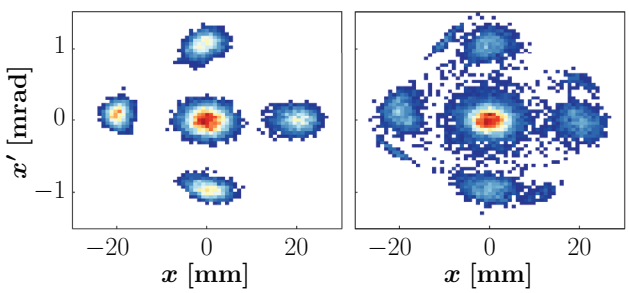

Figure 3: Simulated horizontal phase space portraits at the end of the splitting process in the absence of a tune ripple (left) and with a ripple amplitude corresponding to the maximum measured current ripple on the PFW circuits (right). The efficiency of the splitting process is clearly reduced in the latter case.

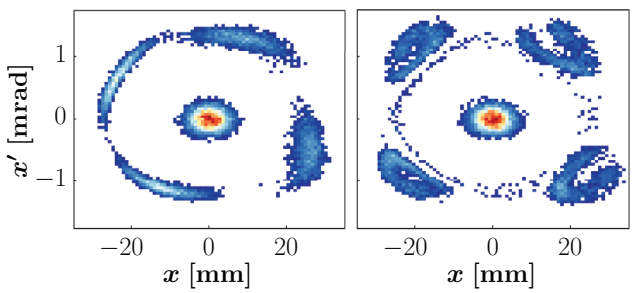

Figure 5: Simulated horizontal phase space portraits during a non-adiabatic final rotation. Once the beamlets are sufficiently separated (see Fig. 3), the rotation occurs within 2000 turns. An intermediate situation after 1000 turns is shown on the left and the phase space on the right corresponds to the end of the rotation process.

ISBN 978-3-95450-178-6

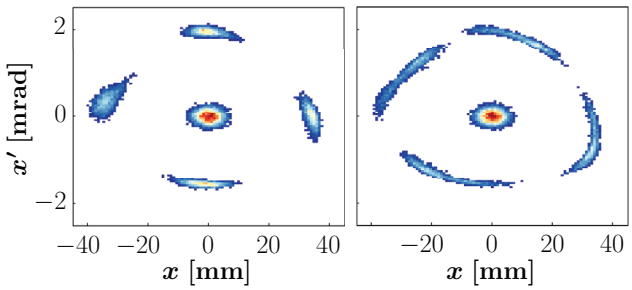

Figure 6: Simulated horizontal phase space portraits showing the evolution of an improved final rotation, which takes about six times longer than the one illustrated in Fig. 5. η_{MTE} is conserved during the process and the final surface of the islands is significantly reduced.

septum is increased and only particles in the tails of the island's distribution are likely to be absorbed.

The changes to the multipolar configuration were experimentally implemented and the extraction efficiency was indeed improved by about 4%. The final step pursued to further increase the extraction efficiency was to correctly position the dummy septum with respect to SMH16, i.e. to establish shadowing conditions. The corresponding experimental results are set out in the following section.

SHADOWING CONFIGURATION

TPS15 has been designed to absorb particles that would otherwise be lost at SMH16 during the rise time of the fast extraction kickers. As this device constitutes an additional aperture restriction in the extraction region, a complete redesign of the extraction bump was required to extract the MTE beam. Experimental studies showed the necessity to move TPS15 to its minimum position of 80.5 mm and an angle of 0 mrad in order to provide sufficient separation between the beam and the septum blade during the extraction process.

Therefore, the remaining degrees of freedom to position SMH16 in the shadow of TPS15 corresponded to the position and angle of SMH16 and a fine scan of these parameters was experimentally conducted to determine the settings, which minimize beam loss in SS16.

By means of a fast beam loss monitor (BLM) in SS16, which allows to resolve beam loss on a time scale shorter than one turn, losses occurring during the extraction of the islands can be distinguished from those created during the final turn. In Fig. 7, a typical beam loss pattern during the last five turns is shown. To evaluate the shadowing efficiency, the sum of the losses occurring for the core and the islands was considered as figure of merit and the dependency of this value on the position and angle of SMH16 was investigated. For an angle of 0 mrad, beam loss was observed to be a quadratic function of the position, with a minimum located at 58.65 mm (see Fig. 7 bottom). The losses measured at this position corresponded to a reduction by about a factor three compared to the value obtained for the settings of TPS15 and SMH16, which were considered operational at the time

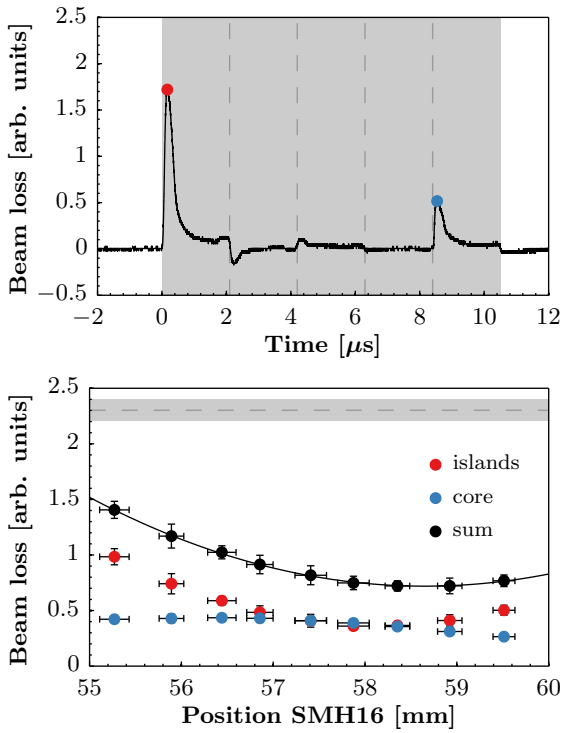

Figure 7: Top: Signal of the fast BLM16. The grey area indicates a duration of five turns, with the dashed lines being separated by one turn. The red and the blue circles correspond to the maximum beam loss occurring during the extraction of the islands and the core, respectively. Bottom: Dependency of beam loss on the position of SMH16 for an angle of 0 mrad. Red and blue circles correspond to the losses of the islands and the core, respectively, and the black circles represent their sum. Error bars describe the standard deviation obtained over 10 consecutive measurements. The dashed line and the grey band indicate mean value and standard deviation of losses for the nominal septa settings.

these measurements were conducted (82.5 mm / 0 mrad and 55.5 mm / 3 mrad, respectively). Based on these results, the following settings were chosen as new operational configuration: TPS15 at 80.5 mm / 0 mrad and SMH16 at 57.5 mm / 1 mrad. These values constitute an acceptable compromise for both MTE and the other operational users.

PERFORMANCE ANALYSIS OF THE 2015 RUN

Based on the increased understanding of the MTE process and the implemented mitigation measures to overcome the issues, which stopped the deployment of MTE in 2010, it became again possible to transfer MTE beams to the SPS at the end of 2015. From September 21$^{\mathrm{st}}$ until the end of the proton run on November 16$^{\mathrm{th}}$, MTE replaced the CT technique. Continuous beam optimisation was carried out, and intensities of up to 2.0×10^{13} p could be operationally extracted.

ISBN 978-3-95450-178-6

the proton run on November 16th, MTE replaced the CT technique. Continuous beam optimisation was carried out, and intensities of up to 2.0×10^{13} p could be operationally extracted.

The striking advantage of MTE over CT is visualized in Fig. 8, where measurements with slow BLMs, which are installed around the PS circumference in the 100 straight sections and integrate beam loss over 1 ms, are presented. Beam loss occurs mainly in the extraction region and activation of the rest of the machine is significantly reduced.

Figure 9 presents the time evolution of the extracted beam intensity and of the extraction efficiency η_{ext}. For MTE, η_{ext} is around 97-98%, whereas typical values for CT at similar beam intensity are around 95%. Hence, MTE reduces extraction losses with respect to CT by almost a factor of 2 and concentrates them in the well-shielded SS15.

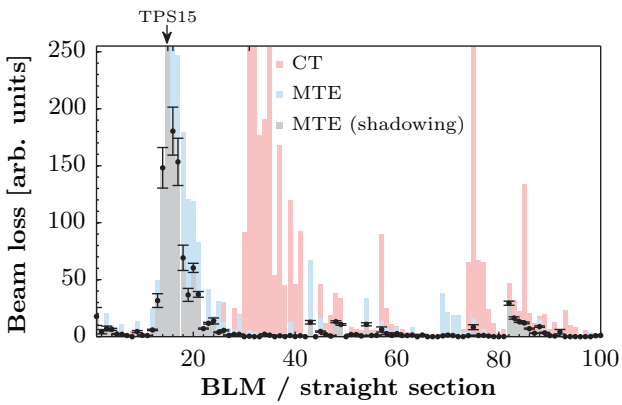

Figure 8: Integrated beam loss measured after extraction on the MTE cycle using TPS15 and SMH16 in shadowing configuration. Only BLM15 is saturated, and beam loss at the adjacent SMH16 is significantly reduced. For comparison, the MTE case without TPS15 and the CT case are shown. Error bars for the case of MTE with shadowing correspond to the standard deviation of 500 consecutive measurements.

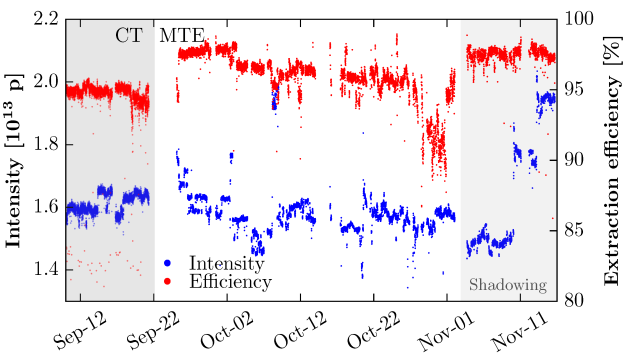

Figure 9: Evolution of the PS proton intensity measured prior to extraction and of η_{ext} during the 2015 MTE run. Operation with CT and the period using the shadowing configuration are highlighted in grey.

A summary of some statistical indicators describing the MTE performance for an intensity of 2.0×10^{13} p is listed in Table 1.

Table 1: Splitting and Extraction Efficiencies for the 2015 MTE Beam with an Intensity of 2.0×10^{13} p. Based on 15×10^3 different measurements, the mean (μ), median (Q_2), and standard deviation (σ) of the two quantities are quoted.

η_{MTE}			η_{ext}		
μ	Q_2	σ	μ	Q_2	σ
19.90	19.92	0.41	97.50	97.56	0.60

RECENT PERFORMANCE IMPROVEMENTS

As a result of the aforementioned performance improvements of the MTE technique and the operational experience gained during the MTE run in 2015, the decision was taken to adopt MTE as the operational extraction scheme throughout the 2016 run.

In parallel to the operational use of MTE, studies are being carried out to further improve the MTE reproducibility. This especially concerns the optimization of the applied multipole functions and of the settings of the wide band stripline kicker of the transverse damper system.

Figure 10 shows that an excitation of at least 20% of the maximum available excitation amplitude is required to properly populate the islands during the splitting process. The transverse splitting also crucially depends on the horizontal emittance before resonance crossing and the transverse damper was found to be efficient in reducing the dependency of η_{MTE} on the initial emittance.

Furthermore, scans of the excitation frequency confirmed that its fractional part is required to be close to 0.25, while η_{MTE} was found to be basically independent of the integer tune value of the excitation frequency.

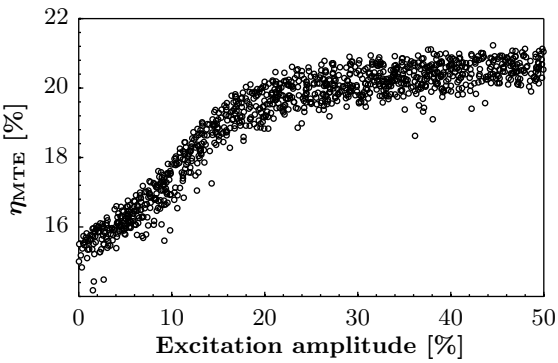

Figure 10: Dependency of the splitting efficiency on the excitation amplitude of the transverse damper (in % of the maximum amplitude). An amplitude of at least 20% is required to achieve proper splitting efficiency.

ISBN 978-3-95450-178-6

REFERENCES

[1] C. Bovet *et al.*, "The Fast Shaving Ejection for Beam Transfer from the CPS to the CERN 300 GeV Machine," IEEE Trans. Nucl. Sci. **20**, 438 (1973).

[2] J. Barranco García and S. Gilardoni, "Simulation and Optimization of Beam Losses During Continuous Transfer Extraction at the CERN Proton Synchrotron," Phys. Rev. ST Accel. Beams **14**, 030101 (2011).

[3] R. Cappi and M. Giovannozzi, "Novel Method for Multiturn Extraction: Trapping Charged Particles in Islands of Phase Space," Phys. Rev. Lett. **88**, 104801 (2002).

[4] M. Giovannozzi, "Status of MTE," Presentation at the LHC Injectors and Experimental Facilities Committee (IEFC) meeting, CERN, Geneva, Switzerland (12 May 2010).

[5] C. Bertone *et al.*, "Studies and Implementation of the PS Dummy Septum to Mitigate Irradiation of Magnetic Septum in Straight Section 16," CERN-ACC-2014-0043 (2014).

[6] J. Borburgh *et al.*, "First Implementation of Transversely Split Proton Beams in the CERN Proton Synchrotron for the Fixed-Target Physics Programme," EPL **113**, 34001 (2016).

[7] P. Freyermuth *et al.*, "CERN Proton Synchrotron Working Point Matrix for Extended Pole Face Winding Powering Scheme," in *Proc. of IPAC10*, Kyoto, Japan (2010).

[8] A.P. Shishlo, T.V. Gorlov, and J.A. Holmes, "The Python Shell for the ORBIT Code," *Proc. of ICAP09*, San Francisco, USA (2009).

[9] F. Schmidt, E. Forest, and E. McIntosh, "Introduction to the Polymorphic Tracking Code: Fibre Bundles, Polymorphic Taylor Types and "Exact Tracking"," CERN-SL-2002-044-AP. KEK-REPORT-2002-3 (2002).

[10] M. Giovannozzi *et al.*, "The CERN PS Multi-Turn Extraction Based on Beam Splittting in Stable Islands of Transverse Phase Space: Design Report," CERN-2006-011 (2006).

ISBN 978-3-95450-178-6